Radio Observations of Weak Coronal Transients

Mukul R. Kundu

Department of Astronomy, University of Maryland, College Park, Maryland 20742, USA
E-mail: kundu@astro.umd.edu

Abstract

In this review we discuss radio observations of weak coronal transients. We concentrate on the transient events observed primarily by Yohkoh/SXT and to a smaller extent by SOHO/EIT. The radio observations are those obtained with the Very Large Array (VLA) in microwaves, the Nancay (France) metric radioheliograph at 150 - 450 MHz and the Nobeyama RadioHeliograph (NRH) at 17 GHz. We discuss the observational characteristics of X-ray bright point flares at meter wavelengths and in microwaves, and provide evidence that both thermal and nonthermal processes occur in these small scale flaring events. Similarly, radio observations of X-ray jets in microwaves and at meter wavelengths provide evidence for both thermal and nonthermal processes in these dynamic coronal phenomena. Nonthermal radio emission in the form of metric type III bursts is produced by electron beams propagating along the jet, whereas microwave emission comes mostly from the jet base. We discuss active region transient brightenings (ARTB's) and show that their radio emission can be purely thermal, thermal gyro- resonance or nonthermal gyrosynchrotron radiation. We discuss one form (radio-selected) of quiet Sun transient brightenings located far from active regions. We provide evidence that weak plasma ejections following flares is observed at metric wavelengths in the form of transient continuum emission. Finally, we discuss the time-varying polar brightenings at 17 GHz, and their relationship to polar erupting plumes observed by SOHO-EIT.

Key words: Sun: corona - Sun: active regions - Sun: X-rays - Sun: radio continuum

1. Introduction

Observations made over the past several years with the soft and hard X-ray telescopes (SXT and HXT) on the Japanese satellite Yohkoh have resulted in many new and important discoveries. For example, they have revealed that the X-ray corona is much more dynamic than had been suspected before. Because of the high spatial resolution and the large dynamic range of SXT, it has been possible to discover varieties of small scale energy releases on the Sun and to study them with extraordinary sensitivity and detail. As a result, we now know of several new phenomena: (a) XBP flares and their extended structures; (b) coronal X-ray jets; (c) Active Region Transient Brightenings (ARTB's); and (d) X-ray plasmoid ejections. Similarly, the SOHO/EIT/SUMER/UVCS experiments have revealed many transients such as eruptive plumes, macro spicules, etc. in EUV images. All these small scale phenomena have their distinctive morphological and physical properties in X-rays, and their interpretations, although related, can take on different variations. Radio observations provide information complementary to that of soft X-ray or EUV images: the latter two are dominated by thermal emission from coronal plasma, whereas radio observations are also sensitive to nonthermal emission and to much cooler plasma. However, radio observations are not always the most efficient way to search for transients because radio observed morphological structures of weak transients take rather simple forms. Hence most radio studies of transients use X-ray selected event lists.

2. XBP Flares

Solar X-ray-bright points (XBPs) are compact emitting regions associated with bipolar magnetic fields. At any one time there appear to be dozens of XBPs present on the Sun. Their lifetimes range from a few hours to several days, although only a small number appear to last longer than 2 days. They may be associated with a large fraction of the magnetic flux that emerges to the solar surface. They are known to flare.

From Skylab data (e.g. Golub et al. 1974) it has been known that about 10% of XBPs exhibit a type of sudden, substantial increase in surface brightness which in larger regions would be termed flaring. These flares appear to be

impulsive in nature, lasting 2-3 minutes. One of the most important aspects of bright point flares, is whether or not XBP flares produce nonthermal populations of energetic particles, as do ordinary flares. The two methods best suited for detecting the presence of nonthermal electron populations are hard X-ray observations and metric-wavelength radio observations. However, the current sensitivity of hard X-ray detectors limits searches for hard X-rays from flaring XBPs. On the other hand, the production of metric radio emission by nonthermal electron beams is very efficient due to the coherent nature of the emission mechanism, and thus such nonthermal electrons might be more easily detectable at radio wavelengths.

Kundu, Gergely, & Golub (1980) used the Clark Lake Radio Observatory interferometer data to look for short-lived type III bursts at the times of flaring bright points identified in the Skylab images. They found only a 10% association between flaring XBPs and type III bursts. The sensitivity of both radio and soft X-ray detectors has improved since these observations. In particular, Yohkoh-SXT has produced excellent images of XBP's on a regular basis with high time and spatial resolution. In the radio domain, there have been two dedicated radioheliographs – the Nancay (France) metric radioheliograph (150 - 450 MHz) and the Nobeyama Radio Heliograph (NRH) at 17 GHz. Kundu et al. (1994a, b) undertook studies of radio emission at meter wavelengths and in microwaves from flaring X-ray-bright points. They took advantage of the improved sensitivity in soft X-rays available with the Yohkoh-SXT telescope (Tsuneta et al. 1991), and the excellent accuracy of source location at metric wavelengths available with the Nancay radioheliograph which can measure burst positions with an accuracy of better than $1'$; in microwaves they used NRH with 10" spatial resolution and time resolution of 1 sec.

2.1. Meter-wave Observations

A search was made for meter-wavelength radio emission from more than a dozen coronal bright points observed in soft X-rays by the Yohkoh/SXT experiment. In all, six of the 20 XBP X-ray brightenings showed evidence for an associated radio burst. The metric radio emissions were type III bursts, which are produced by nonthermal beams of electrons: this represents strong evidence that the XBP-flare mechanism is capable of accelerating particles to nonthermal energies, as well as producing the heated material detected in soft X-rays.

2.1.1. Metric Type III Burst Emission from an XBP Flare in a Coronal Hole

We examined SXT quarter-resolution images prior to (08:32 UT, 1992 June 21) and during (08:41 UT) an XBP flare in a coronal hole along with the metric imaging data. The quiescent soft X-ray emission from this XBP was very weak, and it was barely visible in the image. It lies at the eastern edge of a prominent low-latitude "guitar"-shaped coronal hole which dominates the region around disk center on this day. The XBP existed from at least 22 UT on June 20, and it exhibited fluctuations in brightness from time to time, sometimes approaching levels which would be called XBP flaring. The X-ray flare lasted about 10 minutes: the time of the peak was poorly determined but was close to 08:37 UT. These soft X-ray flares from this XBP typically have temperatures of order 5 MK and peak emission measures of order 10^{46-47} cm^{-5}.

Coincident with the XBP X-ray flare, the Nancay radioheliograph observed type III-like radio emission at 164, 236, and 327 MHz at 08:37 - 08:38 UT. The radio emission peaks at 08:37:30 at all three frequencies. The radio emission lasts only about 10 s at 164 MHz. The brief duration of individual peaks within the profile, their coincidence in time at all frequencies, and the fact that they are seen across a wide frequency range strongly suggest that these bursts are type III's due to beams of nonthermal electrons propagating out through the corona along open magnetic field lines (e.g. Kundu 1965). There appears to be a small dispersion of position with frequency; the highest frequency (327 MHz) is closest to disk center and the XBP, and the lower frequencies are farther away from the center. The dispersion in position with frequency is consistent with the plasma emission process of type III bursts. The type III bursts observed in conjunction with the XBP flare were rather weak, $\sim$ 20 sfu at both 164 and 236 MHz. They had zero or $< 5\%$ polarization. From the measured source size ($\sim 2'$) and flux (21 sfu), it was estimated that the brightness temperature of the type III burst reaches 7 x 10^8 K at 164 MHz (somewhat lower at the higher frequencies): such a brightness temperature requires the presence of a nonthermal population of electrons in the corona.

2.1.2. Metric Type III Bursts from a Flaring XBP Near an Active Region

The flaring behavior in both radio and X-rays can be more complex if the XBP is located close to an AR. Kundu et al. (1995a) investigated the properties of metric type III emission from such a flaring XBP. This XBP was associated with an emerging flux region (EFR) that appeared on June 21 at 09:00 UT and grew in size until 11:40 UT when the XBP and EFR merged. Besides the simple group of type III bursts which occurred at 08:37:30 UT on June 21

and which were associated with the coronal hole XBP, Kundu et al. observed groups of type III bursts, on the same day at various times between 09:00 and 14:28 UT, associated with the XBP near the AR. Their size $\sim 2'$, degree of circular polarization, 10 - 50%, flux $\sim 5 - 36$ sfu, and computed T_b varies between 8.7 x 10^7 and 7.7 x 10^8 K.

Kundu et al. (1994a) demonstrated that isolated XBP flares located in coronal holes can give rise to nonthermal emission in the form of type III-burst emission from electron beams in addition to thermal soft X-ray emission from the thermal plasma. They also provided additional evidence that recurrent type III bursts at metric wavelengths can result from a flaring XBP located near an active region. This conclusion follows from the temporal and spatial associations between the positions of type III bursts and the XBP flares. It is interesting to speculate that radio bursts could have resulted from the interaction between the newly emerging magnetic flux and the XBP. This may be consistent with the fact that XBP fluctuations are possibly due to magnetic reconnection of emerging flux with ambient coronal fields (Strong et al. 1992).

2.2. Microwave Observations of XBP Flares

Using observations made with the Nobeyama radio heliograph (NRH) at 17 GHz and the Yohkoh/SXT experiment, Kundu et al. (1994a) reported the first detection of 17 GHz signatures of coronal X-ray bright points (XBP's). They detected four BP's at 17 GHz out of eight identified in SXT data on 1992 July 31, for which they looked for 17 GHz emission. For one XBP located in a quiet mixed-polarity region, the peak times at 17 GHz and X-rays were very similar, and both were long lasting – about 2 hours in duration. For the quiet region XBP, the gradual, long-lasting and unpolarized emission suggests that the 17 GHz emission is thermal.

Kundu et al. computed several physical parameters – temperature (T_e), volume emission measure (EM), and electron density (N_e) from a pair of Yohkoh/SXT images in the two thinnest filters at 08:13:31 and 08:15:19 UT, approximately 5 hr after the peak of the flaring event (0330 UT). Using these X-ray parameters, they calculated the thermal emission at 17 GHz. The observed values were higher than the calculated ones. There are many uncertainties in the computations of flux values from X-ray parameters as well as from radio maps. The discrepancy between the observed radio fluxes and the calculated values using the parameters obtained from soft X- ray diagnostics may be due to a lower temperature plasma which cannot be detected by SXT but is sensitive to microwave free-free emission. It is unlikely that the discrepancy referred to above is due to a dominant component of nonthermal radio emission at 17 GHz during the XBP flare.

2.3. Large Scale Microwave Structure and Plasma Flow Associated with an XBP Flare

Gopalswamy et al. (1996) observed large-scale radio structure and plasma flow associated with a bright point flare. The microwave emission consisted of a large-scale structure ($\sim$ 135") and a compact ($\sim$ 30") moving source. The large-scale component seems to be the radio counterpart of large-scale loop structures sometimes observed in association with XBP flares. The compact source moved from the location of the XBP flare with a speed of about 60 km s^{-1}, which Gopalswamy et al. interpreted as suggestive of plasma flow. Spatial comparison between the X-ray and radio data shows that the BP flare had different manifestations in the two wavelength domains. The emission peaks in the two wavelength domains did not coincide, which suggests cool plasma flow along the large-scale radio structure. From the temperature and emission measure of the XBP flare plasma they computed the radio flux which was found to be smaller than the observed radio flux. The peak brightness temperature of the large-scale structure was about 3500 K above the quiet Sun, while the compact source had a brightness temperature of up to $\sim$ 7000 K. The total flux over the area covered by the radio BP flare had a peak value of 0.43 sfu. The total flux of the compact source had a peak value of 0.19 sfu. The XBP flare was located at the northern tip of the extended component of the radio source and was of a much smaller size compared to the extended radio component.

The brightness temperatures of the compact source (7000 K) and the large-scale structure (3500 K) can be easily explained as due to free-free emission. However, the absence of soft X-ray emission at the location of these radio sources places constraints on the density and temperature of the plasma that emits radio waves. From considerations of EM at the location of XBP flare, Gopalswamy et al. (1996) concluded that the radio large scale structure must be at a lower temperature than the X-ray emitting plasma. They estimated that the temperature of the large scale loop was 0.24 MK (observed $T_b \sim 3500$ K) assumed optically thin. The above argument also applies for the compact source. Since there is no soft X-ray emission associated with the compact source, it has to be cooler than the X-ray-emitting plasma. For a temperature of 2.4 x 10^5 K, one needs a plasma density of 1.5 x 10^9 cm^{-3} to produce the observed brightness temperature. The compact source may represent cool material of enhanced density or a plasmoid from the reconnection region flowing through the large-scale structure.

3. Radio Observations of Coronal X-ray Jets

Among the many discoveries made by Yohkoh-SXT, X-ray jets stand out as one of the most interesting ones. These X-ray jets are transitory X-ray enhancements with well-collimated motion (Shibata et al. 1992). In many cases, the jets are associated with small flares at or near their foot points and the motion appears to be a real flow of plasma at temperatures of a few million degrees. The properties of the X-ray jets have been summarized by Shibata et al. (1992), Shibata et al. (1994), and Shimojo et al. (1996).

Magnetohydrodynamic simulations of X-ray jets have been carried out by Shibata et al. (1992) and Yokoyama & Shibata (1995, 1996). The simulations were based on the magnetic reconnection model in which two separate magnetic field lines of emerging flux and of pre-existing coronal fields come close together by the rising motion of the emerging flux. Due to finite resistivity there is reconnection of the field lines, and by Joule dissipation magnetic energy is partly released as heat to increase the temperature of the plasma such that it is observed as X-ray jets. Yokoyama & Shibata (1995) could reproduce many of the observed characteristics of X-ray jets. In particular they found two types of interaction between emerging flux and coronal fields, which would result in two morphologically different X-ray jets. The most frequent type is the anemone jet type which occurs when emerging flux appears in a coronal hole where magnetic field lines are vertical or oblique. The other is the two-sided-loop type which occurs when emerging flux appears in a quiet region where magnetic field is almost horizontal. In that case, hot plasma is ejected along the coronal loops away from both sides of the emerging flux. Thus, the oblique-field case corresponds to the anemone-type jet, and the horizontal-field case corresponds to the two-sided-loop type jet. Besides the jet, there also results a closed loop structure at the base of the jet due to the interaction between the emerging flux and pre-existing coronal fields.

One of the questions to be answered is whether the acceleration process associated with reconnection of field lines produces a nonthermal population of electrons along with the heating of the plasma responsible for soft X-ray emissions. As mentioned earlier, radio observations can provide a simple means of identifying nonthermal effects in these events. Aurass et al. (1994), Kundu et al. (1995b) and Raulin et al. (1996) reported the first detection of nonthermal radio emission in the form of metric type III bursts from coronal X-ray jets. It is also important to look for microwave emission for two reasons: (1) to examine how high in energy the nonthermal electron population go; and (2) to search for thermal emission which may result from the heating responsible for soft X-ray emission in the jets. Since microwave emission is known to originate from energetic electrons confined to magnetic loops, this permits us to study the radio properties of both the jet as well as its base which has a loop like structure.

3.1. Meterwave Observations of Jets

Figure 1 shows a jet seen in SXT images (Aug. 16, 1992) in the thin Al filter. The jet seems to be ejected from an XBP which was resolved by the SXT (with pixel resolution of 2.5") into several component sources which had different variabilities with time. The jet reached its maximum intensity (which was rather broad) around 12:37:28 - 12:38:32 UT. The velocity of the jet was about 300 km s^{-1} at 12:37:28 UT and 100 km s^{-1} at 12:38:32 UT, as determined by visual estimates of the apparent motion.

A type III burst occurred at 12:37:50 UT between the two SXT times defining the broad maximum of jet intensity (Fig. 1). We consider this temporal association between the SXT jet and type III to be excellent. The locations of type III sources at 236.6 and 164 MHz are indicated in Figure 1 with crosses. Note that the 164 MHz position is located on the extension of the jet (that is, the jet is not quite visible at that location). The type III burst had brightness temperatures $T_b \sim 3 - 5 \cdot 10^8$ K depending upon the frequency, and it was unpolarized. The X-ray intensity appears to decrease along the jet in a manner consistent with the exponential fall-off found by Shibata et al. (1992).

The association of type III's with jets establishes that the acceleration of electrons to speeds of $\sim$ c/3 (energies some tens of keV) coincides with these plasma flows. The location of type III bursts at the lower frequency (164 MHz) on the invisible or poorly visible part of the jet suggests that the electron density in that part of the jet is adequate to produce plasma radiation, but not high enough for the jet to be visible in soft X-rays. This is consistent with extrapolation of the decreasing density away from the XBP the site of jet origin. Closer to the jet, the density derived from 236.6 MHz type III burst observation (on the plasma radiation interpretation) is only slightly smaller than or even comparable with the density derived at the top of the jet from SXT observations (7 x10^8 cm^{-3}), assuming that the temperature remains constant along the jet.

Since type III emitting electrons propagate along open field lines in dense coronal structures (Wild et al. 1959; Kundu et al. 1983; Kundu et al. 1995b), we should be able to distinguish between the radio signatures of "anemone-type" jets and "two-sided-loop type" jets (Shibata et al. 1994). In the former, we expect normal type III bursts

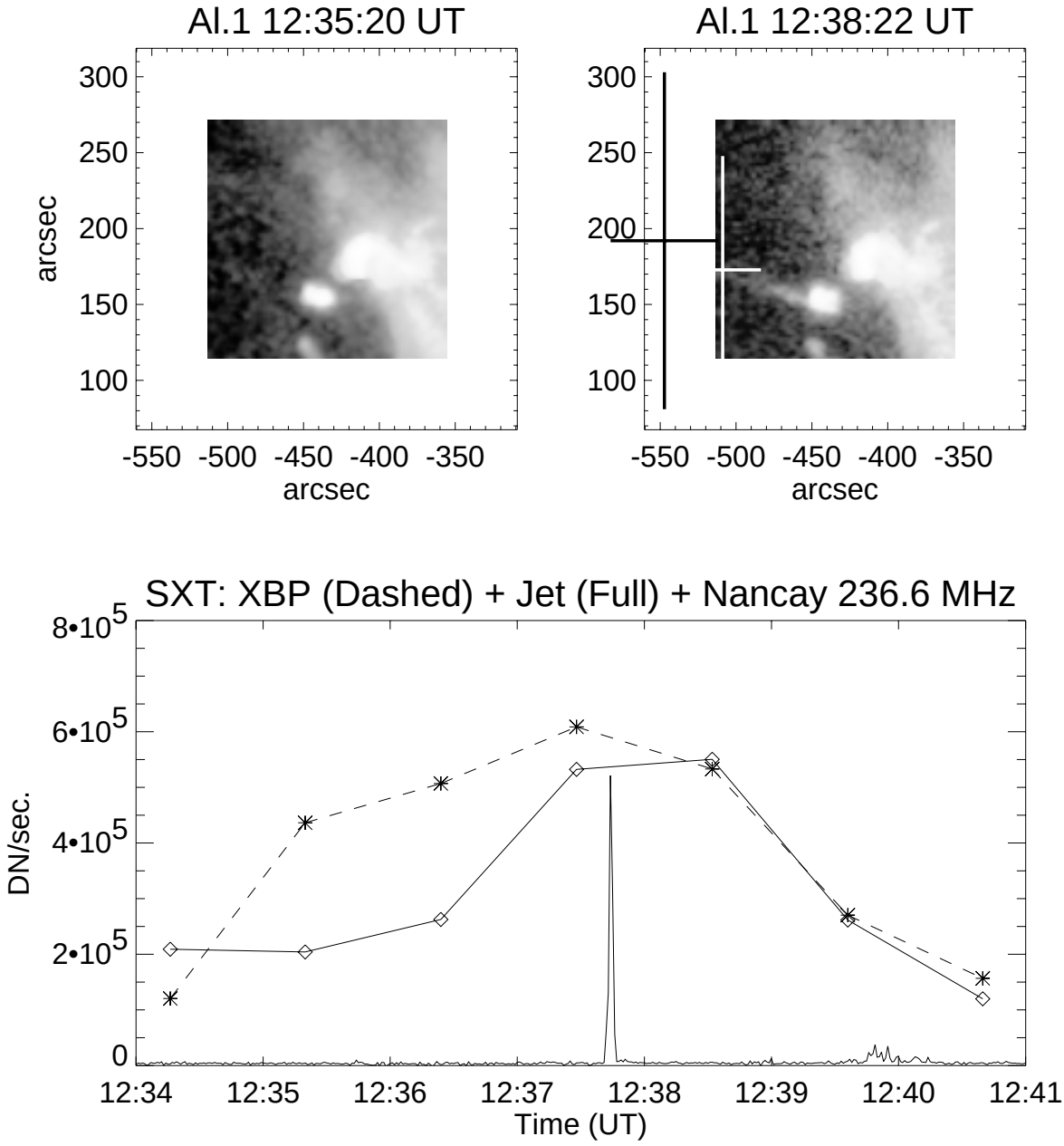

Fig. 1.. (Top) The X-ray jet event shown at two different times, along with the position of type III bursts at 236.6 and 164 MHz. The crosses indicate the E-W and N-S HPBW of the Nancay radioheliograph at 236.6 and 164 MHz. (Bottom) The light curves of the complex of BPs (dashed curves) and of the X-ray jet (solid curves) and the type III burst at 236.6 MHz (From Kundu et al., 1995).

extending over a broad frequency range, whereas in the latter case, where propagation is on low-lying closed field lines horizontal to the photospheric surface, we expect to see type III bursts of very restricted bandwidth, because the type III-producing electron streams will be propagating more or less parallel to equidensity levels of the Sun's atmosphere, and therefore plasma radiation within a limited frequency range will be emitted. We considered 14 well-defined "two-sided-loop" type jets which have the same order of intensity enhancement as the anemone-type jets considered earlier by Kundu et al. (1995b) and Raulin et al. (1996). According to Shimojo et al. (1996), energetically these jets are similar to the anemone-type jets ($\sim 10^{27}$ ergs).

We found that while type IIIs are observed in association with anemone-type jets, we have detected no nonthermal signature in the form of type III bursts for two-sided-loop type jets. This non-detection of type III bursts is consistent with the results of 2-dimensional MHD simulations of soft X-ray jets. The range of jet's plasma density provided by the simulations is 3 - 10 10^9 cm^{-3}, which corresponds to the observed values (Shibata et al. 1994; Kundu et al. 1995b; Raulin et al. 1996). These density values can account for plasma emission at metric wavelengths. However density gradients, which are necessary conditions in order to produce type III bursts, are unlikely to be present in two-sided-loop type jets where the magnetic field resulting from the reconnection process is almost parallel to the photosphere. On the other hand, density gradients are expected in anemone-type jets. Therefore if the reconnection process provides nonthermal particles, we expect fast drift type III bursts (which are produced by ~ 40 keV electrons) to be associated with "anemone" jets but not with "two-sided-loop" jets, as we have observed (Kundu et al. 1998).

3.2. Microwave (17 GHz) Observations of Jets

3.2.1. 1995 March 31 Jet Event

We found that the 17 GHz (unpolarized) microwave emission originates from the base of the jet. Figs. 2a shows some representative partial frame ($5' \times 5'$) images surrounding the jet. The 17 GHz emission at the jet base undergoes changes in time - even the centroid of the emission appears to change (Kundu, Shibasaki, & Nitta, 1997).

In order to show the variation of 17 GHz emission quantitatively, we produced light curves of four areas, using radioheliograph images reconstructed at 10 s intervals (Fig. 3) along with X-ray light curves. These areas are shown in Figure 2. The sources 1-4 for the X-ray light curves are chosen to match the areas for radio light curves. Note that all four sources (1-4) in radio refer to the base (active region loop or loops) from which the X-ray jet emanates. The X-ray light curves for sources 1 and 3 refer to the base, but the light curve "J" corresponds to the jet. A comparison between the two sets of light curves (Fig. 3 in X-ray and 17 GHz) shows that there is only general correspondence between the radio and X-ray emissions from the base sources. The time profiles in the two spectral domains are dissimilar, implying that the sources of microwave and X-rays may not be the same. Although the X-ray jet is not seen at 17 GHz, the base source 2 in radio shows some enhanced activity near the peak of the source "J" in X-rays. The dissimilar behavior of the 17 GHz sources 1 and 2 and of sources 3 and 4 shows that different parts of the jet base evolve independently, although there seems to exist some connection between them. This microwave jet was also associated with a metric type III burst.

3.2.2. 1992 August 25 Jet Event

This jet was observed in the fully developed AR 7260, then located on the west limb. It is characterized by a vertical structure, followed by a roughly horizontal X-ray structure, essentially showing a north-to-west deflection. At 17 GHz, we observe not only the base, but part of the jet (the bottom vertical part) as well. This implies that the lower part of the jet is more optically thick, possibly because of higher electron density, whereas the upper part, as well as the horizontal part (northwest), are optically thin at 17 GHz. The 17 GHz emission is again unpolarized. Fig. 2b shows this jet in X-rays (top) and at 17 GHz (bottom) at similar times.

3.2.3. A Statistical Study of Jets in Microwaves

Nindos et al. (this symposium) made a statistical study of the 17 GHz properties of 18 X-ray coronal jets as observed by the Yohkoh-SXT. They also searched for chromospheric ejecta (Hα surges) during the time intervals when X-ray images were available. Microwave emission was associated with the majority (75%) of the X-ray jets. In agreement with previous results, the radio emission was found to originate from the base or the lower part of the jets. They detected 17 GHz emission from almost all jets which showed flare-like activity at their footpoints. In general, the 17 GHz time profiles were gradual and unpolarized, implying that the emission was thermal. They computed the physical properties of the X-ray emitting plasma jets. In one two-sided-loop type jet and one anemone-type jet, the observed microwave fluxes from the lower part of the jets were well above the fluxes predicted from the computed electron temperatures and emission measures of the soft X-ray-emitting material on the basis of thermal

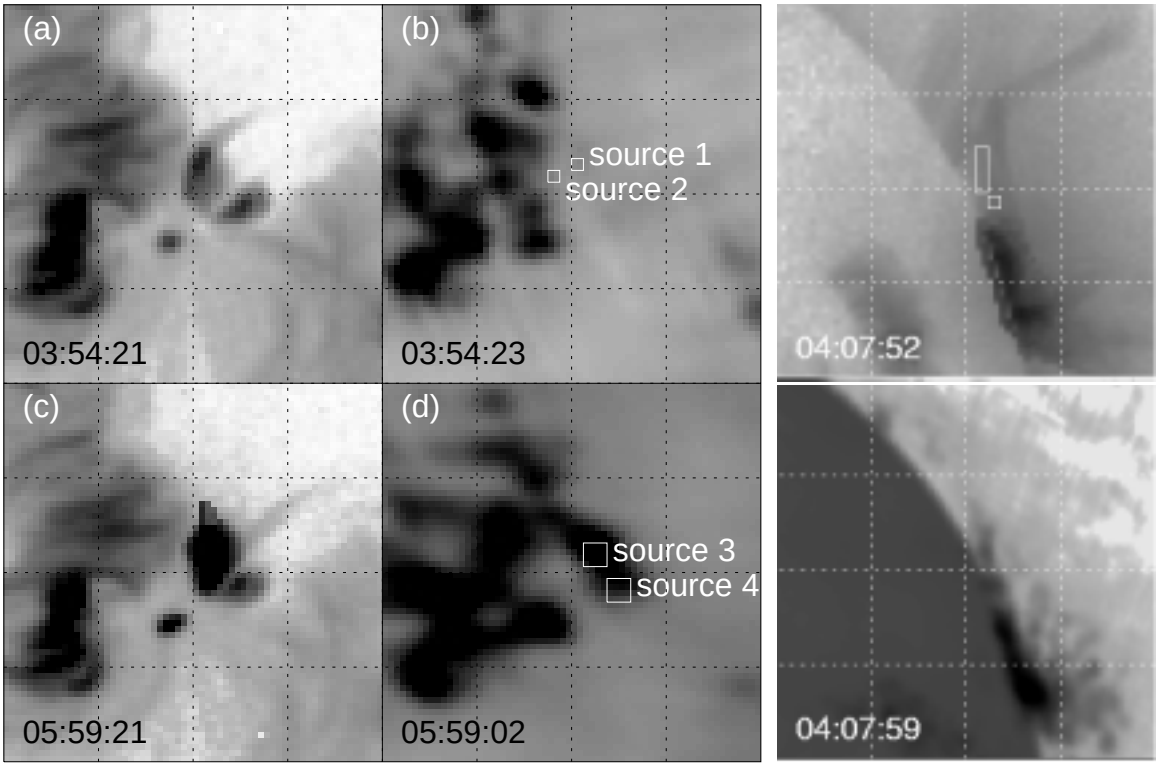

Fig. 2.. a. Representative X-ray (left column) and radio images (middle column) for the jet of March 31, 1995 in which the areas where the light curves of fig. 3 are produced are indicated The field of view of each panel is $\sim 2.2 \times 10^5$ km. b. X-ray (right column, top) and microwave (right column, bottom) images for the jet of August 25, 1992. The field of view of each panel is $\sim 4.4 \times 10^5$ km^2.

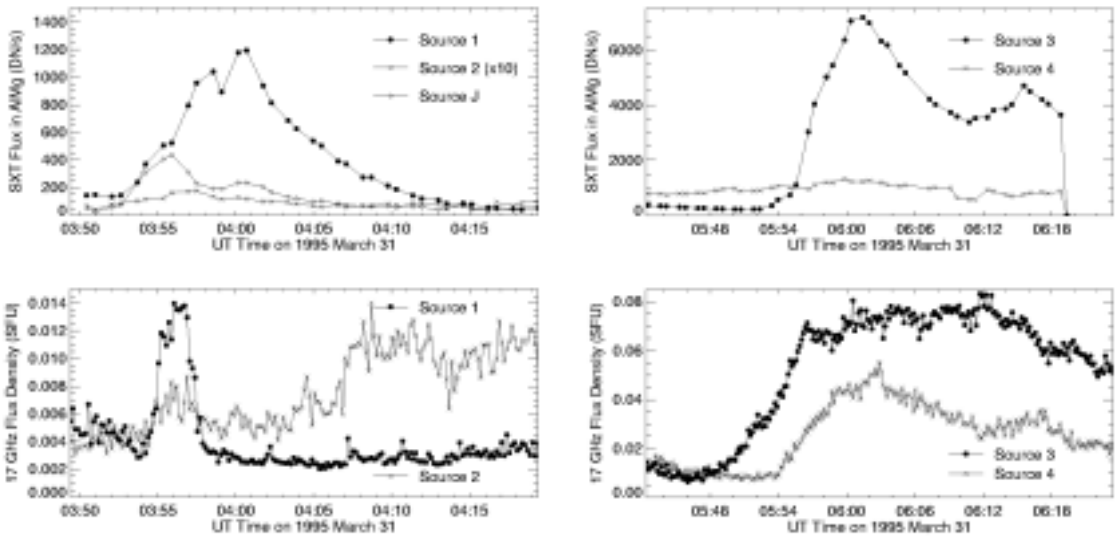

Fig. 3.. Light curves in X-rays and at 17 GHz for the four areas marked in fig. 2a.

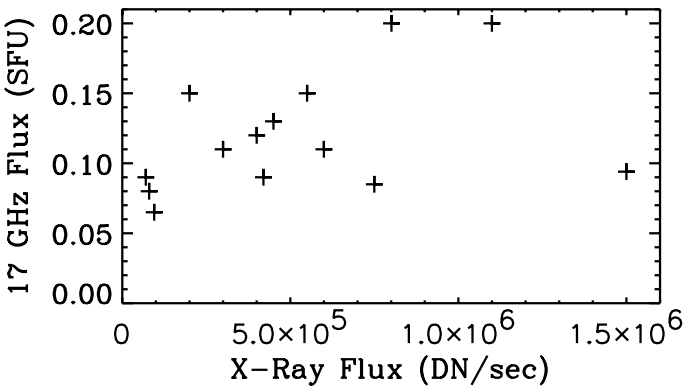

Fig. 4.. Scatter plot between the maximum flux of the X-ray jets and the corresponding maximum 17 GHz flux.

free-free emission. They interpreted these large discrepancies in terms of the presence of lower temperature material which cannot be detected by the SXT but produces strong microwave free-free emission. This is observed in both anemone-type jet (Feb. 9, 1993) and in July 22, 1992 two-sided-loop type jets. No cool material was detected at the base of the jets. They also observed an Hα surge which was not associated with an X-ray jet and showed no signatures on the SXT images but was detected with the NRH. The emission of the microwave surge-associated source was free-free from the chromospheric plasma. Fig. 4 shows a plot of maximum flux of X-ray jets versus the associated 17 GHz flux. As one can see, there is a general correlation between the flux values in the two spectral domains, both being thermal.

3.3. Summary of Radio Studies of Coronal X-Ray Jets

3.3.1. X-ray Jets/Type III Bursts: Nonthermal Processes

The flare-like brightenings associated with jets arising in XBP's are typically too weak to be detectable in hard X-rays, so the radio phenomena must serve to identify any nonthermal effects in these events. We provide evidence that type III bursts are often associated with anemone type X-ray jets and their source positions are aligned along the length of the jets. Existence of type III's provide evidence that nonthermal processes occur in X-ray jets which are produced by a thermal plasma. This implies that particle acceleration occurs in X-ray jets, as is normal in ordinary flares. The type III emission is extremely short-lived relative to the jet process, as can be seen from Fig. 1.

The location of the low frequency type III bursts on the extension of the soft X-ray jet, argues that the coronal jet can be much longer than inferred from soft X-ray measurements. The continuity of jet structure opens the possibility that the electron acceleration may take place considerably lower than the altitude corresponding to the starting frequency of the type III emission. We note that the soft X-ray emission and the radio observing frequency provide two independent means of estimating the electron density at the point of observation. No type III bursts have been detected in association with two-sided-loop type jets because here the magnetic field lines are parallel to the solar surface and type III emitting electrons propagate along open field lines.

3.3.2. X-ray Jets/Microwave Emission: Thermal Processes

We detected microwave (17 GHz) emission from X-ray jets – both anemone as well as two- sided-loop types. The unpolarized 17 GHz emission comes mainly from the base of the jet, although in some cases, the emission seems to originate from the lower part of the jet. The microwave observations imply that the jet is largely optically thin at 17 GHz. 17 GHz emission (unpolarized) occurs in most ($\sim$ 75%) cases. Microwave emission originates from the base of the jet; occasionally it occurs in the lower part of jet. The jet itself must be optically thin at 17 GHz, the jet lower part may sometimes be more optically thick, probably due to higher electron density. It may imply that the field lines containing the X-ray plasma diverge at higher altitudes. The time profiles in the two spectral domains are dissimilar, implying that the areas (loop/loops) producing X-ray and microwave emission may not be the same. 17 GHz emission is observed in two-sided loop type jets as well as anemone type jets.

An important issue to consider is whether the radio emission occurs on open or closed field lines. In the case of 1995 March 31 event, we do not see any 17 GHz emission from the X-ray jet itself. We see only the base of the jet, which obviously implies that microwave emission originates in closed loop or loops. In the 1992 August 25 event, we see the jet base as well as the bottom part of the X-ray jet. This suggests that there is 17 GHz emission from the lower part of the X-ray jet on open field lines. The whole jet need not be seen at 17 GHz if the bottom part of the jet has higher optical thickness than the upper part due to expansion of the field lines at higher altitudes. The microwave and X-ray intensities of the jet bases seem to be reasonably well correlated.

4. Active Region Transient Brightenings (ARTB's)

4.1. X-ray Observations

Shimizu et al. (1992) first reported the frequent occurrence of soft X-ray brightenings in solar active regions. These are easily seen in data from the soft X-ray telescope (SXT; Tsuneta et al. 1991) on board Yohkoh, which is particularly sensitive to such brightenings because of its high spatial resolution and high dynamic range. They last from a few minutes to tens of minutes, correspond to tiny enhancements in the GOES 0.5-4 Å channel, have a thermal energy content in the range 10^{25} - 10^{29} ergs, and their frequency of occurrence (1-40 events per hour per active region) has a strong correlation with the total soft X-ray flux of the active region (Shimizu et al. 1992). Morphologically, they appear about as often in a single loop as in a dual loop configuration, and when they are in a dual loop configuration they often ($\sim$ 60% of events) show a Y shape, indicative of two loops interacting at their nearer legs (Shimizu et al. 1994).

It has been hypothesized that soft X-ray transient brightenings could be the low-energy extension of the general flare distribution. If so, the transient brightenings would extend flares to lower energies by at least 2 orders of magnitude below subflares. Then the transient brightenings would presumably be the soft X-ray counterpart to microflares, discovered by Lin et al. (1984).

4.2. Radio (VLA) Observations

Using the VLA, Gopalswamy et al. (1994) first reported transient brightenings in microwaves (at 2 cm) and their relationship with soft X-ray brightenings observed by Shimizu. These microwave transient brightenings are small-scale energy releases in coronal active regions. They are compact ($\sim$ 2") sources with duration ranging from less than a minute to more than 20 minutes. Their typical microwave flux at 2 cm (0.002 - 0.025 sfu) is nearly 2 orders of magnitude smaller than that from normal flares. They are also highly polarized, sometimes reaching 100%; they are located close to the spotward footpoints of coronal loops connecting the periphery of the sunspot umbra to nearby regions of opposite magnetic polarity.

Two of the VLA radio brightenings were spatially associated with soft X-ray brightenings, although the 15 GHz time profiles did not match the associated soft X-ray time profiles closely. The majority of the VLA radio brightenings were not associated with soft X-ray increases measured by GOES. The high degree of polarization in the VLA radio data and the association with the penumbra suggest that the radio emission in those cases was thermal gyroresonance emission (radiation at low harmonics of the gyrofrequency) in the strong magnetic fields low in the corona near the sunspot, although Gopalswamy et al. (1994) could not rule out the possibility that the emission was nonthermal gyrosynchrotron emission by accelerated electrons (which generally has degrees of polarization lower than 100%). Consistent with the thermal interpretation is the fact that they did not observe radio emission from the whole loop which brightened in soft X-rays, but only from the footpoint anchored in the penumbra, i.e., from the region of strongest magnetic field in the loop.

4.3. Radio (Nobeyama) Observations

Using the NRH imaging data at 17 GHz along with Yohkoh/SXT data, White et al. (1995) made detailed observations of four events in which 17 GHz radio emission was clearly detected. The time profiles of the 17 GHz data were very similar to those of the soft X-ray fluxes, and the 17 GHz flux was very close to that expected from plasma with the temperature (6 - 7 x 10^6 K) and emission measure derived for the soft X-ray-emitting material from filter ratios. No impulsive nonthermal radio emission was detected from any of the four events, although each was at least GOES class B1 in soft X-rays. Weak hard X-rays may have been detected by GRO/BATSE from the strongest of the events, but not from two others.

In all cases the radio emission predicted on the basis of thermal bremsstrahlung emission from the X-ray-emitting material was reasonably close to the peak flux actually observed. Given the uncertainties in both the radio measure-

ments and the derived soft X-ray properties, this agreement suggests that thermal bremsstrahlung is the emission mechanism for the 17 GHz sources. The obvious alternative would be gyrosynchrotron emission from nonthermal electrons accelerated during the brightening, as occurs in solar flares.

4.4. Radio (OVRO) Observations

Gary et al. (1997) used the Owens Valley Radio Observatory (OVRO) Solar Array, operating at 45 frequencies between 1 and 18 GHz, to search for signs of nonthermal electrons associated with ARTB's. The OVRO Solar Array has two advantages for such a study: (1) the frequency range includes the lower frequencies, where significant nonthermal emission should occur; and (2) the broad frequency coverage reduces the possibility of missing events that may have a relatively narrow flux spectrum, and it allows the spectral shape to be used to verify that the emission is nonthermal.

Gary et al. found that the transient brightenings were clearly detected in microwaves in 12 of 34 events (35%), possibly detected in another 17 of 34 events (50%), and only five of 34 events (15%) had no apparent microwave counterpart. The microwave spectra often peak in the range 5-10 GHz (13 of 16 events), and that the microwave spectra of some events show narrowband spectra with a steep low-frequency slope. Gary et al. (1997) concluded that the emission from at least some events is the result of a nonthermal population of electrons, and that transient brightenings as a whole can therefore be identified as microflares, the low-energy extension of the general flare energy distribution.

4.4.1. VLA Observations (Revisited)

As mentioned earlier, Gopalswamy et al. originally believed that the emission mechanism for microwave transients had to be gyroresonance or nonthermal gyrosynchrotron, but not free-free emission. They could not decide between gyroresonance and gyrosynchrotron processes because of the low time resolution (30 s) used in the data analysis. Since then, they performed a detailed analysis of the VLA data with full time resolution (3.3 s) at two wavelengths (2 and 3.6 cm) in order to adequately address the question of the emission mechanism of the transients. They found that nonthermal processes indeed occur during the μ - λ transients. The fast time structure cannot be explained by a thermodynamic cooling time and therefore requires a nonthermal process. The impulsive components imply an energy release rate of $\sim$ 1.3 x 10^{22}ergs s^{-1}, so the thermal energy content of the transients could be less than 10^{24} ergs.

Zhang et al. (1998) used the same data set as Gopalswamy et al. (1994) and extended the study of microwave transients further by using both 2 and 3.6 cm data and a time resolution of 3.3 s. In particular, they took advantage of the dual wavelength observations and determined the three-dimensional structure of the magnetic loop where the microwave transients occur, since the microwave emission at each wavelength outlines one coronal magnetic layer. They inferred that the 2 and 3.6 cm sources were due to the third and second harmonic gyroresonance emission, respectively. Both the 2 and 3.6 cm emission sources were very compact, originating from coronal layers where the magnetic field was about 1800 G and 1500 G, respectively. The projected angular separation between the 2 and 3.6 cm transient sources was about 2"-3" which corresponds to linear separation along the loop between the two centroids of about 3000 km. The derived magnetic field gradient at the bottom of the magnetic loop was about 0.7 G km^{-1}.

5. Quiet Sun Transients

Nindos et al. (1998) studied a set of radio-selected transient brightenings (TB's) as a complement to the more common X-ray selected surveys. They used VLA observations during a period when the Sun was generally quiet. Five small impulsive events were identified in a set of VLA observations at 4.5, 1.5 and 0.33 GHz and compared with soft X-ray images from Yohkoh and EUV images from SOHO/EIT. Four of the events were located at the edges of an active region but one was located 100" away in a quiet region. The time profiles of the radio TBs showed impulsive peaks while the corresponding soft X-ray profiles were gradual. The impulsive radio peaks were up to 35% polarized. Their data favor an interpretation in terms of gyrosynchrotron radiation from mildly relativistic electrons. A small number of nonthermal electrons with spectral index 3 can explain the observed properties of the TBs. Thus nonthermal TBs can be found away from active regions. Two of the microwave TBs also show evidence for type III radio emission at 327 MHz.

The new VLA observations allowed Nindos et al. to study interesting manifestations of TBs that have not been observed before and could not be revealed using soft X-rays observations only, i.e. the excess P-band type III-like

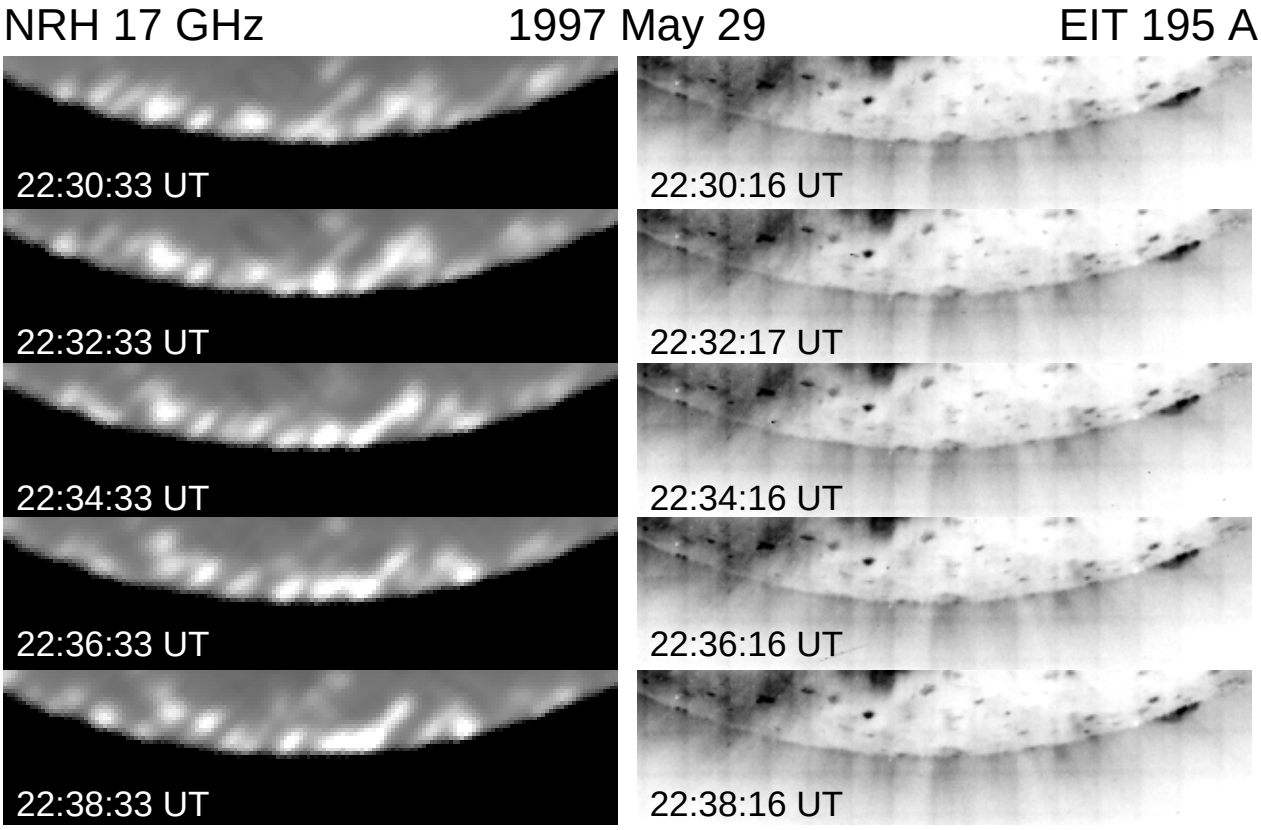

Fig. 5.. A sequence of images of the south pole produced by the Nobeyama Radioheliograph (left column) and SoHO EIT at 195 Å (right column).

emission associated with two TBs and the detection of a TB away from the active region at a location where no steady emission was established from the available data. The detection of a bright nonthermal TB well away from any active region together with the observations of Krücker et al. (1997) show that acceleration of electrons to nonthermal energies can take place even in the quiet solar atmosphere .

6. Soft X-ray Plasma Ejections and Metric Radio Emission (a revisit of type IV)

According to some flare models, impulsive flares result from a magnetic reconnection process, so we would expect a plasma (or plasmoid) ejection to occur above the SXR flaring loop. Shibata et al. (1995) looked for such plasma ejections in association with eight impulsive compact loop flares near the limb, and found that in all cases X-ray plasma ejections occurred above the soft X- ray loops, with an apparent velocity of the ejecta in the range 50-400 Km/s. Since such plasmoids are likely to contain energetic electrons of at least many tens of KeV along with a magnetic field, it is interesting to look for the occurrence of continuum radio events in association with such plasma ejections. We have used the Nancay metric radioheliograph (150- 450 MHz) to look for such continuum events, and in two cases (Feb. 17, 1993 and Nov. 11, 1993) we found continuum emission in the frequency range 164-410 MHz.

7. Transient Radio Emission from Erupting Polar Plumes or Jets

The SOHO/EIT experiments have revealed a new class of explosive events, namely erupting polar plumes or jets. These erupting jets are much more explosive/impulsive than Shibata-type X-ray jets. We have looked for transient radio emission from such jets or erupting plumes using the Nobeyama Radioheliograph at 17 GHz, which is particularly suited to such a study since it takes full-disk images every second. Figure 5(a) shows a sample of images at 17 GHz of the south pole of the Sun made every two minutes in which discrete features can be seen to be

varying with time. We also produced similar images at 10 min. intervals. We have chosen periods when EIT was in high-cadence mode to investigate these features. The advantage of the radio data for a study such as this is that the emission mechanism is well understood, so that the energetics of these events can be addressed. Figure 5(b) shows a sample of EIT images taken every 2 minutes at approximately the same time as the 17 GHz images. One can make two conclusions from these samples of microwave and EUV images. (1) The time varying elements in microwaves and EUV do not have any correspondence. (2) The time varying elements at 17 GHz last shorter than 10 min. but longer than 2 min.

8. Concluding Remarks

We have discussed the radio counterparts of weaker coronal transients as observed primarily in X-rays (Yohkoh/SXT) and to some extent in EUV (SOHO/EIT). We find that in all these transients for which there is a radio counterpart, the radio emission consists of both thermal and nonthermal components. This is true for the transients discussed – XBP flares, coronal X-ray jets, ARTB's, quiet sun transients, and plasma ejections. These transients are at least two orders of magnitude weaker than normal flares both in X-ray and radio domains. Thus, one would like to think of them as microflares with different morphological manifestations in the X-ray domain. In the radio domain, one sees distinct signatures of nonthermal and thermal processes in them. In the case of radio thermal emission, one observes more emission than that computed from the plasma parameters of the thermal X-ray plasma. This may simply imply that the cooler plasma is seen in radio but not in X-rays. We have found no time-coincident microwave counterparts of eruptive polar plumes or similar transient EUV phenomena.

This work at the University of Maryland was supported by NSF grants ATM 96-12738 and INT 97 22489 and by NASA grant NAG 5-6257.

References

Aurass, H., Klein, K. L., and Martens, P. C. H., 1994, Sol. Phys. Lett., 155, 203.
Gary, D. E., Hartl, M., & Shimizu, T., 1997, Astrophys. J., 477, 958.
Golub, L., Krieger, A. S., Vaiana, G. S., Silk, J.K., and Timothy, A.F., 1974, ApJ, 189, L93.
Gopalswamy, N., et al., 1994, ApJ, 437, 522.
Gopalswamy, N., et al., 1996, ApJ, 457, L117.
Gopalswamy, N., Zhang, J., Kundu, M. R., Schmahl, E. J., and Lemen, J. R., 1997, ApJ, 491, L115.
Kundu, M. R., Raulin, J. P., Pick, M., and Strong, K. T., 1995a, ApJ, 444, 922.
Kundu, M. R., Raulin, J. P., and Nitta, N., et al., 1995b, ApJ, 447, L135.
Kundu, M. R., Raulin, J. P., Nitta, N., Shimojo, M., and Shibata, K., 1998, Sol. Phys., 178, 173.
Kundu, M. R., Gergely, T. E., Turner, P. J., and Howard, R. A., 1983, ApJ, 269, L67.
Kundu, M. R., Gergely, T. E., and Golub, L., 1980, ApJ, 236, L87.
Kundu, M. R., Shibasaki, K., and Nitta, N., 1997, ApJ, 991, L121.
Kundu, M. R., Strong, K. T., Pick, M., White, S. M., Hudson, H. S., Harvey, K., and Kane, S. R.,1994a, ApJ, 427, L59.
Kundu, M. R., Shibasaki, K., Enome, S., and Nitta, N., 1994b, ApJ, 431, L155.
Kundu, M. R., 1965, Solar Radio Astronomy, John-Wiley Intersciences Pub.
Krücker, S., Benz, A. O., Bastian, T. S., and Acton, L. W., 1997, ApJ, 488, 499.
Lin, R. P., Schwartz, R. A., Kane, S. R., Pelling, R. M., and Hurley, K. C., 1984, ApJ, 283, 421.
Nindos, A., Kundu, M. R., and White, S. M., 1998, ApJ, in press.
Raulin, J. P., Kundu, M. R., Hudson, H. S., Nitta, N., and Raoult, A., 1996, Astron. Astrophys., 306, 299.
Shibata, K., Ishido, Y., Acton, L.W., et al. 1992, PASJ, 44, L173.
Shibata, K., et al., 1994, "Proc. of Kofu Symposium: A New Look at the Sun" (ed. S. Enome and T. Hirayama), p. 75.
Shibata, K., et al., 1995, ApJ, 451, L83.
Shimizu, T., Tsuneta, S., Acton, L. W., Lemen, J. R., and Uchida, Y., 1992, PASJ, 44, L147.
Shimizu, T., Tsuneta, S., Acton, L. W., Lemen, J. R., Ogawara, Y., and Uchida, Y., 1994, Astrophys. J., 422, 906.
Shimojo, M. et al., 1996, PASJ, 48, 123.
Strong, K. T., et al., 1992, PASJ, 44, L161.
Tsuneta, S., et al., 1991, Sol. Phys., 136, 37.
White, S. M., Kundu, M. R., Shimizu, T., Shibasaki, K., and Enome, S., 1995, Astrophys. J., 450, 435.
Wild, J. P., Sheridan, K. V., and Neylan, A. A., 1959, Aust. J. Phys., 12, 369.
Yokoyama, T., and Shibata, K., 1995, Nature, 375, 42.
Yokoyama, T., and Shibata, K., 1996, PASJ, 48, 3553.
Zhang, J., et al., 1998, Solar Phys., 180, 285.